Sensors and Materials, Vol. 38, No. 2 (2026) 575–580
MYU Tokyo

S & M 4324

Scintillation Properties of CsI Transparent Ceramics

Takumi Kato,[1*] Hiromi Kimura,[2] Taizo Fujiwara,[3] Shuichi Kawasaki,[3]
Daisuke Nakauchi,[1] Noriaki Kawaguchi,[1] and Takayuki Yanagida[1]

[1]Nara Institute of Science and Technology (NAIST), 8916-5 Takayama-cho, Ikoma, Nara 630-0192, Japan
[2]National Metrology Institute of Japan, National Institute of Advanced Industrial Science and Technology (AIST), 1-1-1 Umezono, Tsukuba, Ibaraki 305-8568, Japan
[3]Nihon Kessho Kogaku Co., Ltd., 810-5 Nobe-cho, Tatebayashi, Gunma 374-0047, Japan

(Received October 16, 2025; accepted December 18, 2025)

Keywords: scintillator, CsI, transparent ceramics

CsI transparent ceramics were sintered by the spark plasma sintering method, and their optical and scintillation properties were evaluated. The transmittance was the highest for the CsI transparent ceramic sintered at 200 °C, which was 75% over the 300–800 nm range. The scintillation peaks were mainly observed at 310 nm owing to self-trapped excitons with the decay time constants of 0.03 and ~0.14 μs. The CsI transparent ceramic sintered at 200 °C showed an afterglow level of 150 ppm and light yield of 1700 ph/MeV.

1. Introduction

Scintillation detectors utilize a phosphor material known as a scintillator.[1,2] Scintillators have the ability to promptly convert ionizing radiation into low-energy photons, spanning wavelengths from ultraviolet to visible light. When exposed to ionizing radiation, these scintillators generate electrons and holes and subsequently emit low-energy photons as electrons transition back to their ground states. The emitted photons are then transformed into electrical signals via photoelectric conversion devices, such as photomultiplier tubes or photodiodes, where the signals are amplified for further processing. Scintillation detectors find application in a variety of fields, including medical (e.g., X-ray CT and PET),[3] environmental monitoring,[4] security,[5] and astronomy[6] fields.

The scintillation properties significantly affect detector performance. Generally, a high scintillation light yield (*LY*), a short decay time constant, and high detection efficiency are essential factors.[7] The *LY* and decay time constant, which are luminescence properties of the material, are mainly determined by doping with emission center elements such as rare-earth and transition-metal elements. Enhancing detection efficiency requires materials with high transmittance and a large effective atomic number (Z_{eff}). Owing to the critical importance of translucency in bulk forms, single crystals have traditionally been the most commonly used material for scintillators.[8–10] Single crystal scintillators offer superior translucency and *LY* compared with ceramic counterparts. However, some transparent ceramics exhibit scintillation

*Corresponding author: e-mail: kato.takumi.ki5@ms.naist.jp
https://doi.org/10.18494/SAM6025

ISSN 0914-4935
https://myukk.org/

properties that surpass those of single crystals, prompting us to pursue the development of new transparent ceramic scintillators.[11–13]

Tl- and Na-doped CsI have been widely used for security and nuclear radiation detection because they have attractive properties such as high *LY* (Tl-doped CsI: 50000 photons/MeV), adequate density (4.53 g/cm^3), and high Z_{eff} (54).[14–16] The current material forms of Tl-doped CsI scintillators are basically single crystal or thin film with a needle-like structure, and CsI transparent ceramics can become candidates for next-generation materials. To date, only one study has shown the scintillation properties of transparent ceramics of pure CsI, and there are no results regarding the *LY*s, afterglow levels (*AL*s), and sintering temperature dependence.[17] Therefore, in this study, we present detailed scintillation properties of CsI transparent ceramics.

2. Materials and Methods

Sintering equipment (Sinter Land LabX-100) was used to prepare CsI transparent ceramics by the spark plasma sintering method. In the sintering process, a raw powder of CsI (99.999%, Albemarle) was heated at each temperature (100, 200, 300, and 400 °C) for 3 h while applying a pressure of 45 MPa (Fig. 1). After sintering ended, the temperature was naturally cooled to room temperature. The single crystal (SC) sample of CsI was also used for comparison, the size of which was 5 × 5 × 5 mm^3 (Saint-Gobain).

Following the synthesis, each ceramic sample was polished to a thickness of 1 mm with sandpaper, and their transmittance spectra were evaluated using a spectrophotometer (SolidSpec-3700, Shimadzu). X-ray-induced scintillation spectra were measured using our original setup[18] with the tube voltage and current of 40 kV and 1.2 mA, respectively. X-ray-induced scintillation decay curves and afterglow curves were also recorded using our original system,[19] and X-rays were generated at the applied voltage of 30 kV. To estimate the scintillation *LY*s, the pulse height spectra under irradiation with 662 keV γ-rays from ^{137}Cs were measured using our original setup[18] with a shaping time of 10 μs. Here, the *LY*s of the samples were calculated by comparing the photoabsorption peak with the Pr-doped $Lu_3Al_5O_{12}$ (Pr:LuAG) scintillator (Furukawa), which has an absolute *LY* of 8500 ph/MeV.

3. Results and Discussion

Figure 2 shows transmittance spectra and sample appearances of CsI ceramic samples. The ceramic samples were polished to 1.0 mm. The edge part of the 100 °C sample became clouded, whereas the center part was transparent. The ceramic samples sintered at above 200 °C had uniform transparency. The ceramic samples contained some cracks that formed during the sintering process. They can be reduced by controlling the cooling process and applying pressure. The transmittance spectra were observed at the center part of the ceramic samples. The transmittance was the highest for the 200 °C sample, which was 75% over the 300–800 nm range. An absorption band was detected at 240 nm owing to self-trapped excitons (STEs) or trace impurities.[20,21]

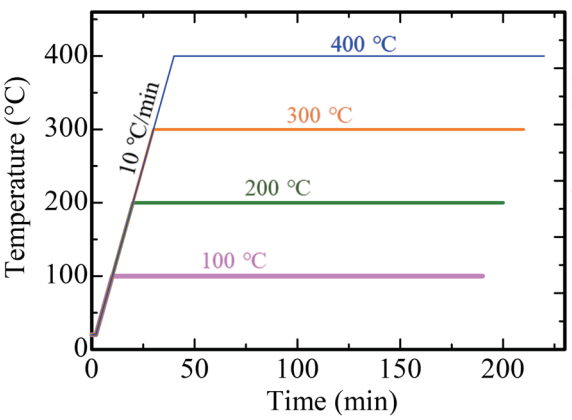

Fig. 1. (Color online) Sintering conditions.

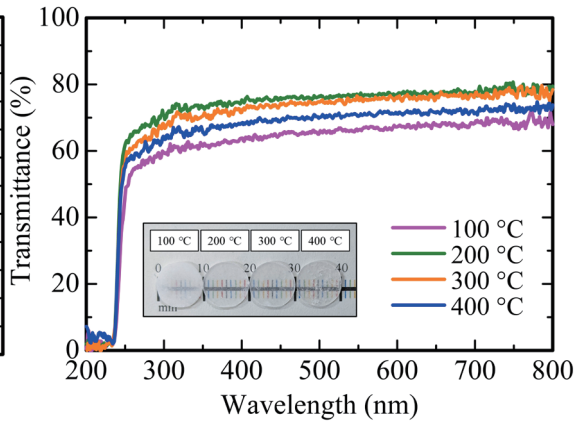

Fig. 2. (Color online) Transmittance spectra and appearances of CsI ceramic samples.

Figure 3 shows scintillation spectra. Scintillation peaks were found in two regions: 200–400 and 400–700 nm. The peak top positions in the 200–400 nm region were consistent with all the samples whether they were ceramics or single crystals, originating from STE.[22] The spectral shapes in the 400–700 nm region were different depending on the samples, and the origins of luminescence have been suggested to be related to trace impurities.[23–25] For instance, the broad emission bands were observed at 550 nm in Tl-doped CsI, 420 nm in Na-doped CsI, and 440 nm in CO_3-doped CsI.[16,26] While no intentional doping with impurities was performed in the present samples, the scintillation peaks in the 400–700 nm region are likely associated with impurities. Figure 4 indicates scintillation decay time profiles and exponential decay curves approximated by the sum of three components. The obtained decay time constants are summarized in Table 1. The first and second constants (τ_1 and τ_2) are attributed to STE, whereas the third (τ_3) is due to luminescence of the trace impurities.[21,22,27]

Figure 5 depicts afterglow profiles. The *AL*s were calculated in the same manner as described in our previous study.[28] *AL* increased as the sintering temperature increased, resulting from point defects that occurred with surface diffusion, grain-boundary diffusion, and volume diffusion at high sintering temperatures. The afterglow level of the 400 °C sample reached a value similar to that of the SC sample. Therefore, the synthesis temperature is considered to affect the number of defect centers. Single crystals are synthesized at temperatures above the melting point, whereas ceramics are sintered at temperatures below the melting point. As a result, it is conceivable that the afterglow level of the single crystal is the highest. Figure 6 shows pulse height spectra of all the samples and Pr:LuAG using the radioisotope of ^{137}Cs. The photoabsorption peaks were observed for all the samples. The *LY*s of CsI transparent ceramics estimated from the photoabsorption peak of Pr:LuAG were comparable to that of the single crystal. The synthesis temperature of the ceramic samples is lower than that of the SC sample, potentially suppressing the formation of defect centers that reduce the energy transfer efficiency. A slight decreasing trend was observed in the *LY*s of the transparent ceramics. This is due to the decreased energy transfer efficiency with sintering at a high sintering temperature, judging from the increasing trend in the *AL*s.

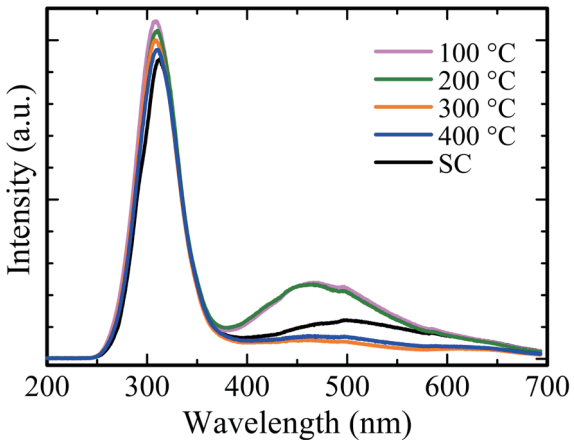

Fig. 3. (Color online) Scintillation spectra. The scintillation intensity is normalized at 310 nm.

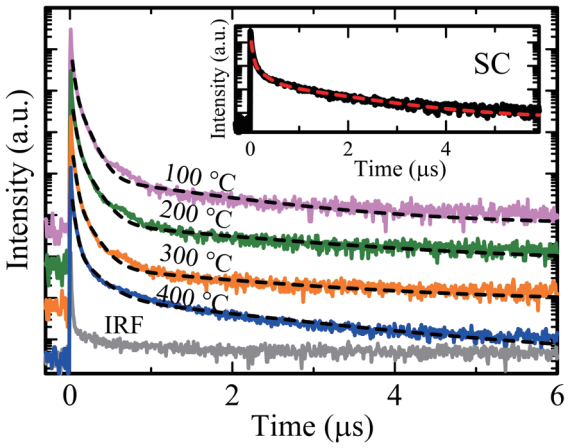

Fig. 4. (Color online) Scintillation decay time profiles.

Table 1
Scintillation decay time constants, afterglow levels, and light yields.

Sample	Decay time constant			*AL* (ppm)	*LY* (ph/MeV)
	τ_1 (μs)	τ_2 (μs)	τ_3 (μs)		
100 °C	0.02	0.09	1.37	130	1700
200 °C	0.03	0.13	2.05	150	1700
300 °C	0.03	0.13	1.97	160	1500
400 °C	0.03	0.18	1.82	230	1400
SC	0.03	0.18	1.27	230	1600

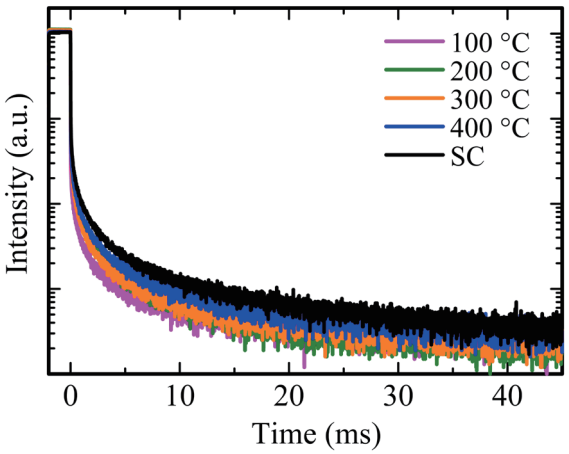

Fig. 5. (Color online) Afterglow profiles.

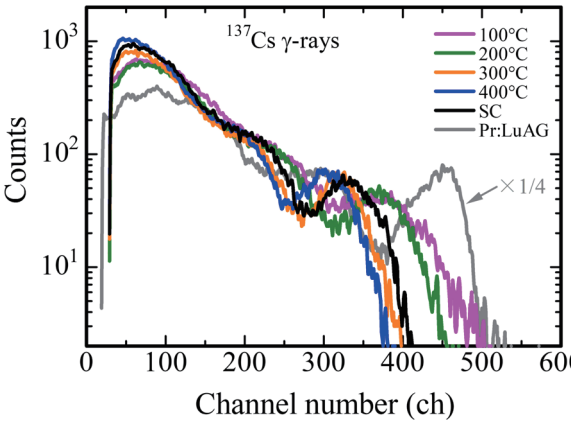

Fig. 6. (Color online) Pulse height spectra under 137Cs γ-ray irradiation.

4. Conclusions

In this study, we revealed the scintillation properties of CsI transparent ceramics. Depending on the sintering temperature, the behavior of luminescence in the 400–700 nm region differed. In common with all the samples, STE luminescence was observed at 310 nm

in the scintillation spectra. The lower sintering temperature led to superior *AL*s and *LY*s for CsI transparent ceramics. The *LY*s of CsI transparent ceramics were comparable to that of the single crystal. From the viewpoint of uniformity and scintillation performance, the CsI transparent ceramic sintered at 200 °C was the most promising among all the samples.

Acknowledgments

This work was supported by the Cooperative Research Project of the Research Center for Biomedical Engineering, Nippon Sheet Glass Foundation, and Hosokawa Powder Technology Foundation.

References

1 T. Yanagida, T. Kato, D. Nakauchi, and N. Kawaguchi: Jpn. J. Appl. Phys. **62** (2023) 010508. https://doi.org/10.35848/1347-4065/ac9026
2 N. Kawaguchi, T. Kato, D. Nakauchi, and T. Yanagida: Jpn. J. Appl. Phys. **62** (2023) 010611. https://doi.org/10.35848/1347-4065/ac99c3
3 C. W. E. van Eijk: Nucl. Instrum. Methods Phys. Res., Sect. A **509** (2003) 17. https://doi.org/10.1016/S0168-9002(03)01542-0
4 K. Watanabe: Jpn. J. Appl. Phys. **62** (2023) 010507. https://doi.org/10.35848/1347-4065/ac90a5
5 J. M. Hall, S. Asztalos, P. Biltoft, J. Church, M. A. Descalle, T. Luu, D. Manatt, G. Mauger, E. Norman, D. Petersen, J. Pruet, S. Prussin, and D. Slaughter: Nucl. Instrum. Methods Phys. Res., Sect. B **261** (2007) 337. https://doi.org/10.1016/j.nimb.2007.04.263
6 K. Yamaoka, M. Ohno, Y. Terada, S. Hong, J. Kotoku, Y. Okada, A. Tsutsui, Y. Endo, K. Abe, Y. Fukazawa, S. Hirakuri, T. Hiruta, K. Itoh, T. Itoh, T. Kamae, M. Kawaharada, N. Kawano, K. Kawashima, T. Kishishita, T. Kitaguchi, M. Kokubun, G.M. Madejski, K. Makishima, T. Mitani, R. Miyawaki, T. Murakami, M.M. Murashima, K. Nakazawa, H. Niko, M. Nomachi, K. Oonuki, G. Sato, M. Suzuki, H. Takahashi, I. Takahashi, T. Takahashi, S. Takeda, K. Tamura, T. Tanaka, M. Tashiro, S. Watanabe, T. Yanagida, and D. Yonetoku: IEEE Trans. Nucl. Sci. **52** (2005) 2765. https://doi.org/10.1109/TNS.2005.862778
7 M. Ishida, A. Watanabe, H. Kawamoto, Y. Fujimoto, and K. Asai: Sens. Mater. **37** (2025) 607. https://doi.org/10.18494/SAM5482
8 K. Ichiba, T. Kato, D. Nakauchi, N. Kawaguchi, and T. Yanagida: Sens. Mater. **36** (2024) 451. https://doi.org/10.18494/SAM4752
9 K. Yamabayashi, K. Okazaki, D. Nakauchi, T. Kato, N. Kawaguchi, and T. Yanagida: Sens. Mater. **36** (2024) 523. https://doi.org/10.18494/SAM4760
10 K. Miyazaki, D. Nakauchi, Y. Takebuchi, T. Kato, N. Kawaguchi, and T. Yanagida: Sens. Mater. **37** (2025) 575. https://doi.org/10.18494/SAM5430
11 T. Kato, G. Okada, K. Fukuda, and T. Yanagida: Radiat. Meas. **106** (2017) 140. https://doi.org/10.1016/j.radmeas.2017.03.032
12 Y. Usui, T. Kato, N. Kawano, G. Okada, N. Kawaguchi, and T. Yanagida: J. Lumin. **200** (2018) 81. https://doi.org/10.1016/j.jlumin.2018.03.008
13 T. Kato, N. Kawano, G. Okada, N. Kawaguchi, K. Fukuda, and T. Yanagida: Optik. **168** (2018) 956. https://doi.org/10.1016/j.ijleo.2018.04.082
14 P. Schotanus, R. Kamermans, and P. Dorenbos: IEEE Trans. Nucl. Sci. **37** (1990) 177. https://doi.org/10.1109/23.106614
15 J. I. Collar, N. E. Fields, M. Hai, T. W. Hossbach, J. L. Orrell, C. T. Overman, G. Perumpilly, and B. Scholz: Nucl. Instrum. Methods Phys. Res., Sect. A **773** (2015) 56. https://doi.org/10.1016/j.nima.2014.11.037
16 P. Yang, C. D. Harmon, F. P. Doty, and J. A. Ohlhausen: IEEE Trans. Nucl. Sci. **61** (2014) 1024. https://doi.org/10.1109/TNS.2014.2300471
17 S. Sen, P. S. Sarkar, G. D. Patra, S. G. Singh, M. Ghosh, S. Pitale, A. N. Patil, and M. K. Pal: Ceram. Int. **47** (2021) 2187. https://doi.org/10.1016/j.ceramint.2020.09.057
18 T. Yanagida, K. Kamada, Y. Fujimoto, H. Yagi, and T. Yanagitani: Opt. Mater. **35** (2013) 2480. https://doi.org/10.1016/j.optmat.2013.07.002

19 T. Yanagida, Y. Fujimoto, T. Ito, K. Uchiyama, and K. Mori: Appl. Phys. Express **7** (2014) 062401. https://doi.org/10.7567/APEX.7.062401
20 C. Bates, A. Salau, and D. Leniart: Phys. Rev. B **15** (1977) 5963. https://doi.org/10.1103/PhysRevB.15.5963
21 V.I. Goriletsky, L.G. Eidelman, A. N. Panova, K. V Shaki-Iova, L. N. Shpilinskaya, L. Vinograd, and A. I. Mitichkin: Nucl. Tracks Radiat. Meas. **21** (1993) 109. https://doi.org/10.1016/1359-0189(93)90055-E
22 H. Nishimura, M. Sakata, T. Tsujimoto, and M. Nakayama: Phys. Rev. B **51** (1995) 2167. https://doi.org/10.1103/PhysRevB.51.2167
23 M. Moszyński, A. Syntfeld-Kazuch, L. Swiderski, P. Sibczyński, M. Grodzicka, T. Szczęśniak, A. V. Gektin, P. Schotanus, N. Shiran, and R. T. Williams: IEEE Trans. Nucl. Sci. **63** (2016) 459. https://doi.org/10.1109/TNS.2015.2509071
24 Z. Wu, B. Yang, and P. D. Townsend: J. Lumin. **128** (2008) 1191. https://doi.org/10.1016/j.jlumin.2007.11.091
25 B. K. Utts and S. E. Spagno: IEEE Trans. Nucl. Sci. **37** (1990) 134. https://doi.org/10.1109/23.106605
26 V. Yakovlev, L. Trefilova, A. Lebedinsky, Z. Daulet, and I. Dubtsov: J. Lumin. **173** (2016) 34. https://doi.org/10.1016/j.jlumin.2015.12.044
27 A. V Gektin, I. M. Krasovitskaya, N. V. Shiran, V. V. Shlyahturov, and E. L. Vinograd: IEEE Trans. Nucl. Sci. **42** (1995) 285. https://doi.org/10.1109/23.467835
28 Y. Endo, K. Ichiba, D. Nakauchi, T. Kato, N. Kawaguchi, and T. Yanagida: Sens. Mater. **36** (2024) 473. https://doi.org/10.18494/SAM4758